Frost, Ray L. & Palmer, Sara J. (2011) ***A Raman and infrared spectroscopic study of the mineral delvauxite CaFe3+4(PO4,SO4)2(OH)8•4-6H2O- a 'colloidal' mineral.*** Spectrochimica Acta Part A : Molecular and Biomolecular Spectroscopy, 78(4), pp. 1250-1254.

A Raman and infrared spectroscopic study of the mineral delvauxite $CaFe^{3+}_4(PO_4,SO_4)_2(OH)_8 \cdot 4\text{-}6H_2O$- a 'colloidal' mineral

Ray L. Frost • and Sara J. Palmer

Chemistry Discipline, Faculty of Science and Technology, Queensland University of Technology, GPO Box 2434, Brisbane Queensland 4001, Australia.

Abstract

The mineral delvauxite $CaFe^{3+}_4(PO_4,SO_4)_2(OH)_8 \cdot 4\text{-}6H_2O$ has been characterised by Raman spectroscopy and infrared spectroscopy. The mineral is associated with the minerals diadochite and destinezite. Delvauxite appears to vary in crystallinity from amorphous to semi-crystalline. The mineral is often X-ray non-diffracting. The minerals are found in soils and may be described as 'colloidal' minerals. Vibrational spectroscopy enables determination of the molecular structure of delvauxite. Bands are assigned to phosphate and sulphate stretching and bending modes. Two symmetric stretching modes for both the phosphate and sulphate symmetric stretching modes support the concept of non-equivalent phosphate and sulphate units in the mineral structure. Multiple water bending and stretching modes imply that non-equivalent water molecules in the structure exist with different hydrogen bond strengths.

Keywords: delvauxite, destinezite, diadochite, phosphate, sulphate, Raman spectroscopy.

• Author to whom correspondence should be addressed (r.frost@qut.edu.au)

1. Introduction

The mineral delvauxite is a hydrated hydroxy phosphate of ferric iron with some sulphate substitution for phosphate, thus giving the following formula: $CaFe^{3+}_4(PO_4,SO_4)_2(OH)_8 \cdot 4\text{-}6H_2O$ [1, 2]. Its name was previously known as borickite. The mineral has been identified in many parts of the world including Australia from the St. John's quarry, near Kapunda, Mount Lofty Ranges, South Australia. Delvauxite is one of several minerals found in caves and is of a formula which is perhaps ill defined [3, 4]. The mineral forms stalagtites. The mineral is amorphous and has been referred to as a colloidal mineral and this no doubt defines why the composition of the mineral is open to question at least in terms of the number of waters of hydration. The molecular structure of the mineral is unknown. There is a need to increase our fundamental knowledge of this mineral as it is an important mineral found in soils and functions as a sink for phosphate and sulphate.

The mineral is yellowish brown to reddish to brownish black and all colours in-between. Delvauxite may ion exchange with many cations and as a consequence the colour varies. The mineral is X-ray non-diffracting. The mineral is diagenetically related to destinezite $Fe^{3+}_2(PO_4,SO_4)_2(OH)\cdot 6H_2O$, which is triclinic. The amorphous form of destinezite is known as diadochite $Fe^{3+}_2(PO_4,SO_4)_2(OH)\cdot 5H_2O$. These minerals are formed through the reaction of acid sulphate solutions with already formed phosphate minerals. Because of the unknown and ill-defined structure of this mineral, it is important to undertake structural studies. As the mineral is amorphous, the application of vibrational spectroscopy is very important.

Raman spectroscopy has proven very useful for the study of minerals [5-11]. Indeed Raman spectroscopy has proven most useful for the study of diagenetically related minerals as often occurs with minerals containing sulphate and phosphate groups, including delvauxite, diadochite and destinezite. Delvauxite is a poorly described mineral, which is generally found as amorphous brown botryoidal crusts and masses in iron ores. Raman spectroscopy is especially useful when the minerals are X-ray non-diffracting and is very useful for the study of amorphous minerals such as delvauxite. This paper is a part of systematic studies of vibrational spectra of minerals of secondary origin in the oxide supergene zone. In this work we attribute bands at various wavenumbers to vibrational modes of delvauxite using Raman spectroscopy and relate the spectra to the structure of the mineral.

2. Experimental

2.1 Mineral

The mineral was supplied by the Mineralogical Research Company and the mineral originated from Berneau, near Vise, Liège, Belgium. The amorphous nature of the mineral was confirmed by X-ray powder diffraction and the chemical analyses determined using an electron probe.

2.2 Raman spectroscopy

Crystals of delvauxite were placed on a polished metal surface on the stage of an Olympus BHSM microscope, which is equipped with 10x, 20x, and 50x objectives. The microscope is part of a Renishaw 1000 Raman microscope system, which also includes a monochromator, a filter system and a CCD detector (1024 pixels). The Raman spectra were excited by a Spectra-Physics model 127 He-Ne laser producing highly polarised light at 633 nm and collected at a nominal resolution of 2 cm^{-1} and a precision of ± 1 cm^{-1} in the range between 100 and 4000 cm^{-1}. Repeated acquisition on the crystals using the highest magnification (50x) were accumulated to improve the signal to noise ratio in the spectra. Spectra were calibrated using the 520.5 cm^{-1} line of a silicon wafer.

2.3 Infrared spectroscopy

Infrared spectra were obtained using a Nicolet Nexus 870 FTIR spectrometer with a smart endurance single bounce diamond ATR cell. Spectra over the 4000–525 cm^{-1} range were obtained by the co-addition of 64 scans with a resolution of 4 cm^{-1} and a mirror velocity of 0.6329 cm/s. Spectra were co-added to improve the signal to noise ratio.

Band component analysis was undertaken using the Jandel 'Peakfit' (Erkrath, Germany) software package which enabled the type of fitting function to be selected and allowed specific parameters to be fixed or varied accordingly. Band fitting was done using a Lorentz-Gauss cross-product function with the minimum number of component bands used for the fitting process. The Lorentz-Gauss ratio was maintained at values greater than 0.7 and

fitting was undertaken until reproducible results were obtained with squared correlations (r^2) greater than 0.995. Band fitting of the spectra is quite reliable providing there is some band separation or changes in the spectral profile.

3. Results and Discussion

3.1 Background

Delvauxite is chemically related to destinezite at least in formula $(Fe^{3+}_2(PO_4,SO_4)_2(OH)\cdot 6H_2O)$. The mineral destinezite is a hydrated hydroxy phosphate of ferric iron with some sulphate substitution of formula $Fe_2(PO_4,SO_4)_2(OH)\cdot 6H_2O$ with the iron in the ferric state [12-15]. The mineral [14] is triclinic with cell parameters = 9.584Å, b = 9.748Å, c = 7.338Å, $\alpha = 93.07°$, $\beta = 95.78°$, $\gamma = 105.32°$. According to Peacor *et al.* [14] the crystal structure consists of infinite chains of $Fe(O,OH,H_2O)_6$ octahedra, sulphate tetrahedra and phosphate tetrahedra linked by a unique system of vertex sharing. The chains are weakly bonded into layers by hydrogen bonding between OH and H_2O of the Fe(III) octahedra and oxygen ions of the sulphate tetrahedra [14]. Layers of tetrahedral/octahedral chains alternate with sheets of H_2O molecules. Peacor *et al.* [14] state that the structure resembles hydrated clay minerals, with H_2O molecules that act as hydrogen bond donors and acceptors to oxygen atoms of adjacent slabs. The mineral has a clay-like appearance under the SEM. The amorphous form of the mineral is called diadochite and is commonly regarded as a colloidal mineral [13, 16-18].

The authors have recently investigated the Raman and infrared spectra of destinezite, and have assigned bands to sulphate and phosphate stretching and bending vibrations. Raman bands observed at around 980 cm^{-1} were assigned to the ν_1 $(PO_4)^{3-}$ symmetric stretching modes, bands at around 1050 cm^{-1} were assigned to the ν_1 $(SO_4)^{2-}$ symmetric stretching modes, while bands between 1180 and 1400 cm^{-1} were assigned to the combination of ν_3 $(PO_4)^{3-}$ and $(SO_4)^{2-}$ antisymmetric stretching modes. Lower wavenumber bands observed for destinezite were assigned to bending modes of sulphate and phosphate. Raman bands observed at around 615 cm^{-1} were assigned to the ν_4 $(SO_4)^{2-}$ bending modes, bands at around 565 cm^{-1} were assigned to ν_4 $(PO_4)^{3-}$ bending modes, while bands centred at around 450 cm^{-1} were assigned to the ν_2 $(SO_4)^{2-}$ bending modes. These band positions agree well with values

reported by Ross [12], who has completed numerous studies on sulphate and phosphate minerals.

3.2 Raman and infrared spectroscopy

The amorphous nature of the mineral is reflected in the Raman and infrared spectra as the spectra are broad and ill defined. The Raman spectra in the 900 to 1500 cm^{-1} range and the and infrared spectra in the 825 to 1325 cm^{-1} range are displayed in Figures 1a and 1b. This region is the spectral region where the sulphate and phosphate stretching vibrations are to be found. Raman bands are observed at 968, 1005, 1033 and 1280 cm^{-1}. The probable attribution of these bands is as follows: the band at 968 cm^{-1} is assigned to the $\nu_1 (PO_4)^{3-}$ symmetric stretching mode, the two bands at 1005 and 1033 cm^{-1} are attributed to $\nu_1 (SO_4)^{2-}$ symmetric stretching modes, while the broad Raman band at 1280 cm^{-1} is assigned to the combination of $\nu_3 (PO_4)^{3-}$ and $(SO_4)^{2-}$ antisymmetric stretching modes. The observation of two sulphate symmetric stretching modes suggests that there are two non-equivalent sulphate units in the mineral structure. The intensity and breadth of this band indicates the coupling of sulphate and phosphate antisymmetric stretching modes. The infrared spectrum also shows a lack of spectral features. Two shoulders at 1046 and 1137 cm^{-1} are observed. The spectral profile was curve fitted and component bands observed at 921, 988, 1046, 1095, 1137, 1167 and 1191 cm^{-1}. The fitting process is somewhat arbitrary as the spectral features are minimal. However, the infrared bands at 988 and 1046 cm^{-1} may be assigned to the $\nu_1 (PO_4)^{3-}$ and $(SO_4)^{2-}$ symmetric stretching modes, while the infrared bands at 1095, 1137, 1167 and 1191 cm^{-1} are assigned to the $\nu_3 (PO_4)^{3-}$ and $(SO_4)^{2-}$ antisymmetric stretching modes.

The Raman spectrum of delvauxite in the 325 to 725 cm^{-1} range and the infrared spectrum in the 525 to 825 cm^{-1} range are displayed in Figure 2. This spectral region is where the phosphate and sulphate bending modes are found. Raman bands are observed at 386, 467, 485, 588, 633 and 656 cm^{-1}. Ross [19] investigated the infrared spectrum of selected sulphate minerals and reported the $\nu_4 SO_4^{2-}$ bending modes at 595, 618 and 680 cm^{-1}. Ross [19] also reported that the infrared spectrum of römerite observed the $\nu_2 (SO_4)^{2-}$ bending modes at 460 and 494 cm^{-1}. Thus the Raman bands at 588, 633 and 656 cm^{-1} are assigned to the $\nu_4 SO_4^{2-}$ bending modes. The first band at 588 cm^{-1} may also be due to the $\nu_4 PO_4^{3-}$ bending modes.

The bands at 467 and 485 cm^{-1} may be assigned to the $\nu_2 (SO_4)^{2-}$ bending modes, while the band at 386 cm^{-1} is possibly the $\nu_2 PO_4^{3-}$ bending mode. In the infrared spectrum, bands are found at 595, 681, 692, 756, 780 and 799 cm^{-1}. The infrared band at 595 cm^{-1} is assigned to the $\nu_4 PO_4^{3-}$ bending mode. The two infrared bands at 681 and 692 cm^{-1} are due to the ν_4 SO_4^{2-} bending modes, while the infrared bands at 756, 780 and 799 cm^{-1} are attributed to water librational modes. The observation of multiple librational modes supports the concept of non-equivalent water units in the mineral structure.

The Raman spectrum of delvauxite in the low wavenumber region between 75 and 325 cm^{-1} is displayed in Figure 3a and the infrared spectrum in the 1400 to 1800 cm^{-1} region in Figure 3b. Intense Raman bands are observed at 144, 155, 214 and 275 and 285 cm^{-1}. It is thought that the latter three bands are related to water hydrogen bonds, while the first two bands are simply described as lattice vibrations. Figure 3b displays the infrared spectrum of the water bending vibration. Two bands are resolved at 1595 and 1659 cm^{-1}. The first band is assigned to water bending modes of non-hydrogen bonded water and the second band at 1659 cm^{-1} to strongly hydrogen bonded water. The observation of two water bending modes is in harmony with the two librational modes.

The Raman and infrared spectra of the OH stretching region is shown in Figures 4a and 4b. The Raman spectrum suffers from low signal to noise. This is not unexpected since water has a very low Raman scattering cross-section. Raman bands are observed at 2900, 3029, 3193 and 3317 cm^{-1}. These bands are ascribed to water stretching vibrations. The variation in the position of the bands fully supports the concept of water with a range of hydrogen bonding. The infrared spectrum displays a broad spectral profile and infrared bands are resolved at 2957, 3195, 3407 and 3535 cm^{-1}. Thus, the spectra correspond well with one another. The higher wavenumber bands in the infrared spectra (3407 and 3535 cm^{-1}) are assigned to OH stretching vibrations.

4. **Conclusions**

The question must be asked: is the mineral delvauxite a unique mineral. Delvauxite has been described as an example of a ‘colloidal’ mineral. Such a question cannot be answered by XRD, however, Raman spectroscopy goes someway to characterising the delvauxite mineral structure. The weak intensity and broadness of the bands indicates the amorphous nature of

delvauxite. Raman and infrared bands have been assigned to sulphate and phosphate stretching and bending modes. The position of the bands corresponded well with the position of bands observed for destinezite and diadochite. Multiple stretching and bending modes for sulphate, phosphate and water indicates that non-equivalent sulphate, phosphate and water units exist in this mineral.

Acknowledgements

The financial and infra-structure support of the Queensland University of Technology Chemistry Discipline of the Faculty of Science and Technology, is gratefully acknowledged. The Australian Research Council (ARC) is thanked for funding the instrumentation.

205 **References**

206

207 [1] E. Dittler, Z. Chem. Ind. Kolloide, 5 (1910) 35.

208 [2] J. Vala, R. Helmhacker, Jahrbuch fur Mineralogie, (1875) 317.

209 [3] X. Stainer, A Deposit of Delvauxite and of Manganese at Couthuin, Mem., (1909) 3-12.

210 [4] K.A. Vakusevich, Zapiski Vser. Min. Ob., 76 (1947) 271-272.

211 [5] R.L. Frost, S. Bahfenne, J. Raman Spectrosc., 41 (2010) 207-211.

212 [6] R.L. Frost, S. Bahfenne, J. Raman Spectrosc., 41 (2010) 325-328.

213 [7] R.L. Frost, S. Bahfenne, J. Cejka, J. Sejkora, S.J. Palmer, R. Skoda, J. Raman Spectrosc.,

214 41 (2010) 690-693.

215 [8] R.L. Frost, S. Bahfenne, J. Cejka, J. Sejkora, J. Plasil, S.J. Palmer, J. Raman Spectrosc.,

216 41 (2010) 814-819.

217 [9] R.L. Frost, K.H. Bakon, S.J. Palmer, J. Raman Spectrosc., 41 (2010) 78-83.

218 [10] R.L. Frost, J. Cejka, J. Sejkora, J. Plasil, S. Bahfenne, S.J. Palmer, J. Raman Spectrosc.,

219 41 (2010) 571-575.

220 [11] R.L. Frost, J. Cejka, J. Sejkora, J. Plasil, S. Bahfenne, S.J. Palmer, J. Raman Spectrosc.,

221 41 (2010) 566-570.

222 [12] V. Bouska, E.K. Lazarenko, Y.M. Melnik, E. Slanski, Acta Univ. Carolinae, Geol.,

223 (1960) 127-152.

224 [13] L.D. German, Zapiski Vser. Min. Ob., 85 (1956) 574-577.

225 [14] D.R. Peacor, R.C. Rouse, T.D. Coskren, E.J. Essene, Clays and Clay Minerals, 47

226 (1999) 1-11.

227 [15] R. Sitzia, Facolta di Scienze dell'Universita di Cagliari, 36 (1966) 105-115.

228 [16] M. Foldvari, B. Nagy, Foldtani Kozlony, 115 (1985) 123-131.

229 [17] M.Z. Fursova, Izvest. Akad.Nauk Kazak.Ser. Geol., 22 (1965) 74-76.

230 [18] A.I. Ginzburg, Trudy Min. Muzeya, Akademiya Nauk SSSR, (1952) 36-63.

231 [19] S.D. Ross, Inorganic Infrared and Raman Spectra (European Chemistry Series), 1972.

232

233

234

235
236
237
238

List of Figures

254

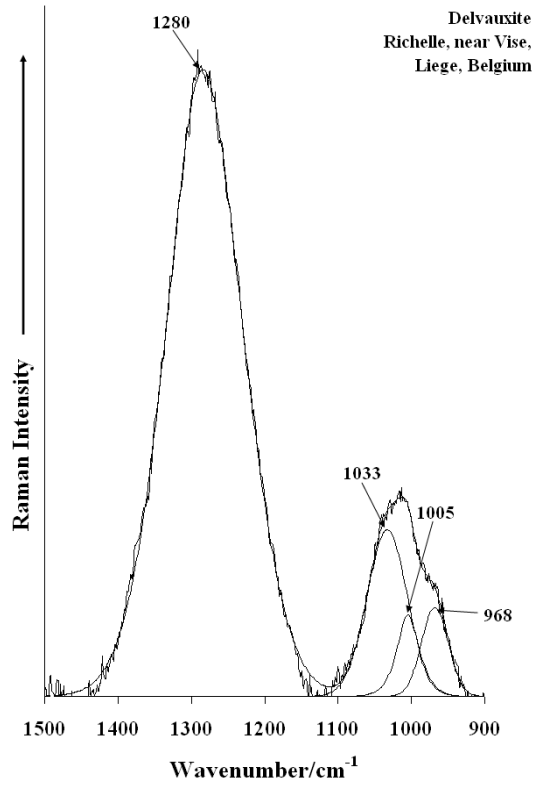

Figure 1a

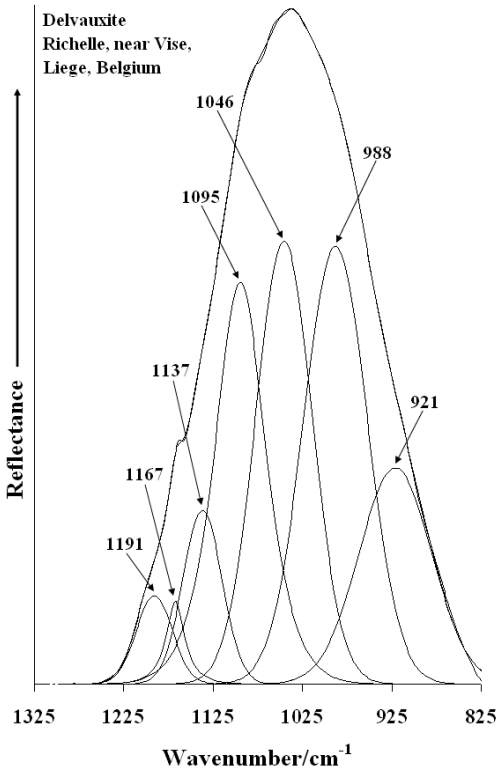

Figure 1b

255
256
257
258

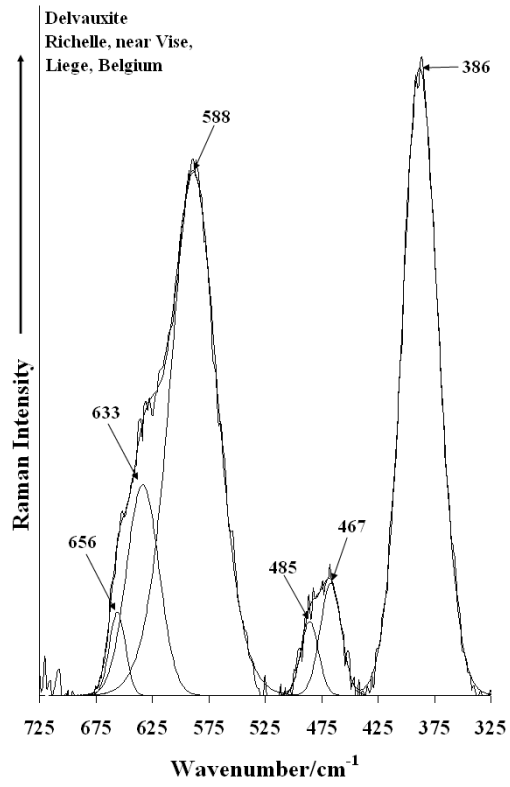

Figure 2a

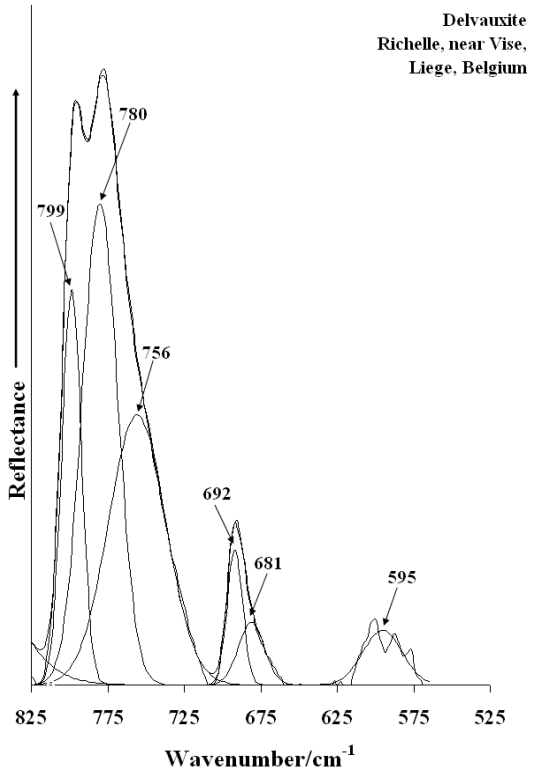

Figure 2b

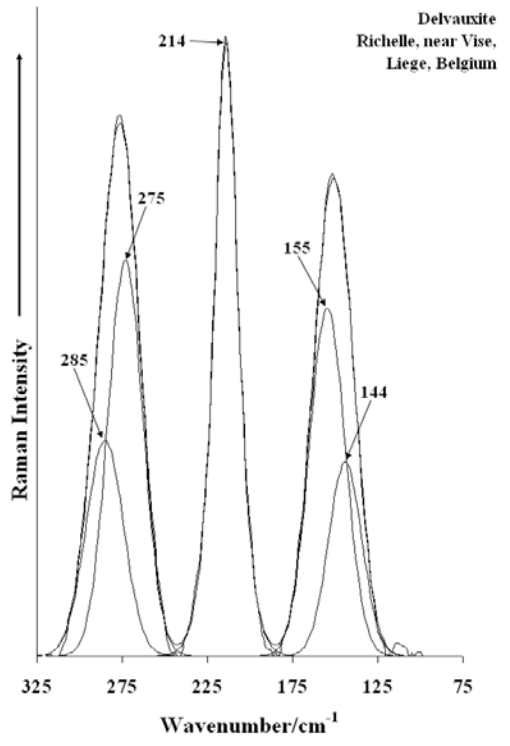

Figure 3a

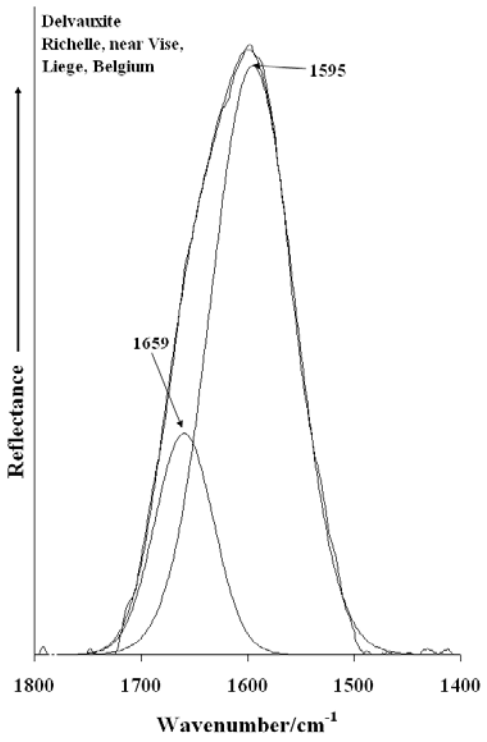

Figure 3b

269

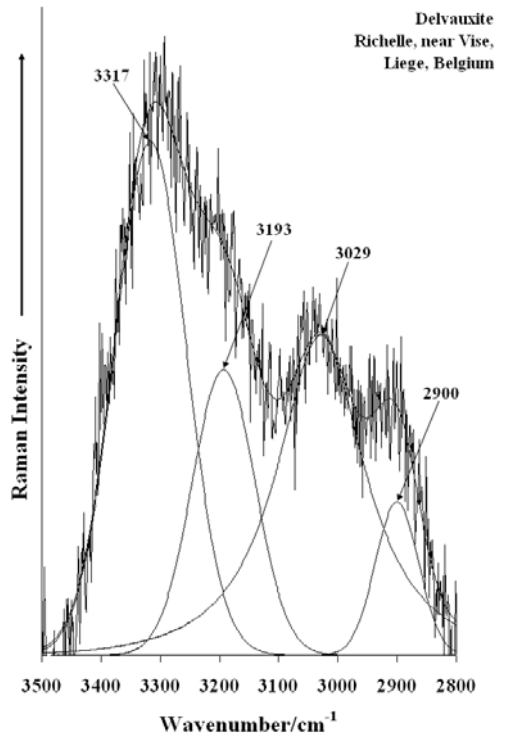

Figure 4a

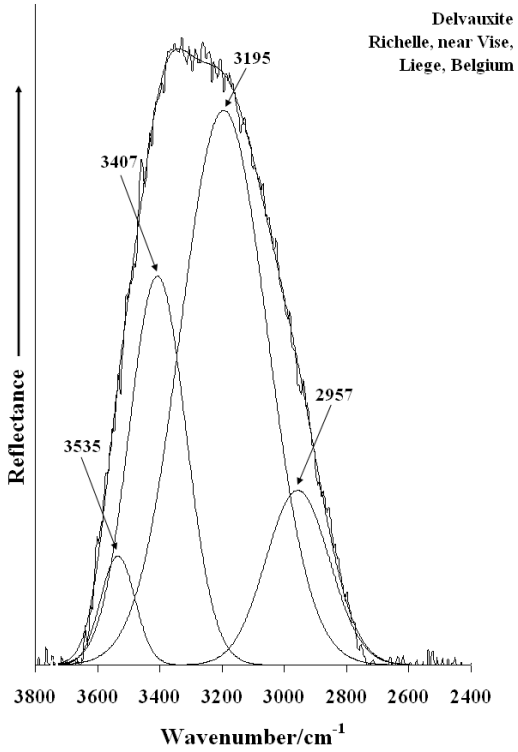

Figure 4b

270
271
272
273
274
275
276
277